Energy Management in Cellular HetNets Assisted by Solar Powered Drone Small Cells

Ahmad Alsharoa[1], Hakim Ghazzai[2], Abdullah Kadri[2], and Ahmed E. Kamal[1]
[1]Iowa State University (ISU), Ames, Iowa, United States,
Email: {alsharoa, kamal}@iastate.edu
[2]Qatar Mobility Innovations Center (QMIC), Qatar University, Doha, Qatar,
Email: {hakimg, abdullahk}@qmic.com

***Abstract*—This paper proposes an energy management framework for cellular heterogeneous networks (HetNets) supported by dynamic drone small cells. A 3-tier HetNet is considered where macrocell, on/off switching micro cells, and solar-powered drone small cells are deployed to serve the networks' subscribers. In addition to energy harvesting, the drones can power their batteries via a charging station located at the macrocell site. Pre-planned locations are identified by the mobile operator for possible drones' placement. The objective of the framework is to optimally determine the positioning of the drones in addition to the micro cells that can be turned off in order to minimize the daily energy consumption of the network. The framework takes also into account the cells' capacity and quality of service (QoS) metric defined by the minimum received power. An integer linear programming problem is formulated to optimally determine the network status during a time blocked period. An online scheme solving the optimization problem is proposed where the future system statistics are unknown. The performances of this online scheme are shown to be very close to those of an ideal benchmark scenario where future network's statistics are perfectly estimated.**

***Index Terms*—Energy harvesting, energy management, heterogeneous networks, dynamic drone small cells.**

I. Introduction

Recently, the use of unmanned aerial vehicles (UAVs), also known as drones, as small cell base stations (BSs) to support ground cellular networks has received considerable attention. Drone base station (DBS) can act as an aerial BS characterized by a quick and dynamic deployment [1], which is extremely helpful for different scenarios. For instance, in public safety communication, where ground infrastructure is damaged by natural disasters, DBSs represent an alternative solution for mobile operators to maintain coverage and connectivity. In fact, DBSs are more robust against such environmental changes thanks to their mobility. DBSs are also useful for temporary/unexpected high traffic demand situations where already deployed infrastructure becomes overloaded and requires additional communication equipment to maintain the high quality-of-service (QoS) level. For example, in big events such as Footbal games, Olympic games, or Concerts, it is unfeasible from economical perspective to invest in the ground infrastructure for a relatively short time period.

Few works in the literature investigate the deployment of the DBSs and its challenges. In [2], a placement technique that uses the drones as relays for cell overloading and outage compensation is proposed. Although they provided an analytical model for evaluating system performance in the downlink direction, the authors did not discuss the DBSs' coverage performance and did not suggest any deployment method. The authors in [3] discussed the optimal deployment position for drones that maximizes the average data rate while keeping the symbol error rate under a certain level. However, their work is limited to only one relaying drone. In [4], the authors analyzed the optimal altitude of one DBS for a certain coverage area that minimizes the DBS's transmit power. Moreover, they investigated the coverage of two DBSs positioned at a fixed altitude and interfering with each other over a certain coverage area.

Recharging the DBSs is another challenging issue in UAV-based communications since traditional wired charging methods are not always feasible. Therefore, energy harvesting (EH) techniques can be considered as one of the most effective and robust solutions to protract the lifetime and sustainability of drones [5]. In general, many promising practical applications that use EH nodes have been discussed such as emerging ultra-dense small cell deployments, point-to-point sensor networks, cognitive radio networks, and far-field microwave power transfer [6]. In UAV-based communications, EH is also considered as an attractive technology for DBSs by offering additional energy to charge their batteries [7]–[9].

In this paper, we investigate the placement of multiple EH DBSs that support typical heterogeneous networks (HetNets) consisting of a single macrocell and multiple micro cells. The proposed method can be generalized in the context of large-scale HetNets. The objective of the framework is to exploit the mobility and quick deployment of the solar powered drones to support the ground cells whenever it is required and when the drones' batteries allow. Inactive drones are placed at a charging station located at the macrocell site. We formulate a binary linear optimization problem aiming at optimally minimizing the total energy consumption in a time block system. During each time block, the proposed approach selects specific drones to be placed at specific potential pre-planned locations. Furthermore, it determines the status of micro cells that can be turned off to save additional energy. This HetNet green operation is managed while taking into account several factors including a QoS metric, the cells' capacity, drones' battery capacity, photovoltaic generation, and the power consumption related to drones' mobility. The performances of this online block-by-block framework are compared to those of an ideal offline benchmark scenario where future network's statistics are perfectly pre-estimated.

This work was made possible by grant NPRP # 6-001-2-001 from the Qatar National Research Fund (a member of The Qatar Foundation). The statements made herein are solely the responsibility of the authors.

II. System Model

In this study, we investigate a time-blocked system of a finite period of time divided into $b = 1, .., B$, blocks of equal duration T_b. The time blocks are relatively long as compared to the channel coherence time and hence, we focus on the system performance based on the average statistics of the network. Investigating the system performance for instantaneous channel realizations and network statistics is not valid for this framework since we are considering the drones' flying time (seconds) which is very large as compared to the channel coherence time (milliseconds).

A. Network Model

We consider downlink transmission in a typical HetNet consisting of one macrocell BS and M $(k = 1, \cdots, M)$ micro cell BSs (MBSs). The HetNet is assisted by D dynamic drones that act as DBSs (i.e., each small BS is carried by one drone) as depicted in Fig. 2.

In this work, we aim to optimize the deployment of DBSs in the considered network according to its need and QoS requirement. We assume that the dynamic drone can be in three different states 1) the drone is in an idle mode and placed at the charging station assumed to be located in the center of the cell (i.e., in the macrocell BS site.), 2) the drone is placed at a pre-defined location in the cell and acts as a DBS to serve users, or 3) the drone is in motion and flying from a location to another. Placing the charging station at the center of the cell minimizes, in general, the flying time of drones and hence the corresponding energy consumption.

We assume that there are $Z+1$ possible locations available for drones' deployment. These locations, $i = 0, \cdots, Z$, can be pre-determined by the mobile operator during the planning phase. Each location i is identified by its 3D geographical coordinates (x_i, y_i, h_i). The location $i = 0$ (i.e., $x_0 = y_0 = h_0 = 0$) corresponds to the charging station. Hence, the drone power consumption depends essentially on its current location (i.e., time block b) and the previous one (i.e., time block $b-1$). We denote by $\boldsymbol{\epsilon^b}$ a binary matrix of size $D \times (Z+1)$. Its entries $\epsilon^b_{d_l}(i)$ indicates the location of the drone d_l, where $l = 1, \cdots, D$. In other words, $\epsilon^b_{d_l}(i) = 1$ if the drone d_l is placed at location i, and $\epsilon^b_{d_l}(i) = 0$ otherwise.

On the other hand, a dynamic on/off switching mechanism is considered to turn off redundant MBSs whenever it is possible [10]. More specifically, MBS $m_k, k = 1, \ldots, M$ can be turned off during low traffic periods and the small number of active users are offloaded to nearby DBSs or macrocell BS. As a result, the energy consumption of lightly loaded MBSs can be reduced or completely eliminated. A binary vector, denoted by $\boldsymbol{\pi}^b$, is introduced to indicate the status of each ground MBS m_k where $\pi^b_{m_k} = 1$ if MBS m_k is operating during time block b, and $\pi^b_{m_k} = 0$ otherwise. It should be noted that we always keep the macrocell BS active to ensure coverage and minimum connectivity in this typical HetNet (i.e., one macrocell BS surrounded by multiple of MBSs). In the case of multiple macrocell BSs covering a bigger geographical area, macrocell BSs can be turned off and cell breathing mechanisms can be employed to ensure connectivity [8].

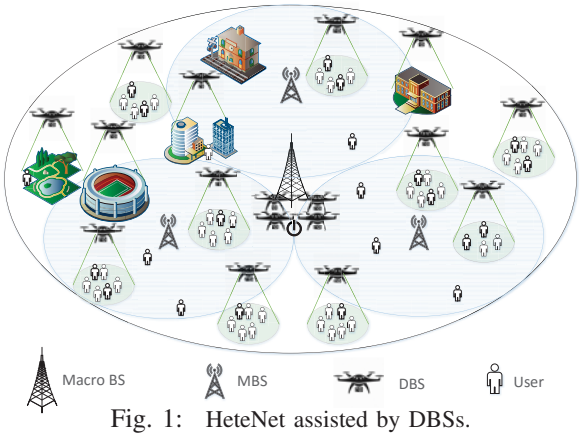

Fig. 1: HeteNet assisted by DBSs.

We denote by U^b the average total number of users located in the macrocell during time block b and by $\bar{U}_0$, $\bar{U}_m$, and $\bar{U}_d$ the maximum number of users served by macrocell BS, MBS m_k, and DBS d_l, respectively, such that $\bar{U}_d \leq \bar{U}_m \ll \bar{U}_0$. These numbers reflect the BSs' capacities due to available number of frequency carriers and/or hardware and transmit power limitations. We assume that the co-channel interference is ignored and the transmissions are performed in orthogonal basis. Also, we assume that a user is served by at most one BS (either a macrocell BS, MBS, or DBS). We consider that the user distribution during time block b over the macrocell area $\mathcal{A}$ follow a certain probability density function (pdf) denoted by $f(x, y, b)$, where (x, y) represents the geographical coordinates of a user. We denote by $\mathcal{A}_\mathcal{X} (\mathcal{A}_\mathcal{X} \subseteq \mathcal{A})$ the coverage area of an active BS $\mathcal{X}$ where $\mathcal{X} \in \{\{0\}, \{m_k : k = 1, \cdots, M\}, \{(d_l, i) : l = 1, \cdots, D, i = 0, \cdots, Z\}\}$ referring to the macrocell BS, MBS m_k and DBS d_l placed at location i, respectively. Hence, the average number of users served by an active BS $\mathcal{X}$ during time block b is denoted by $U^b_\mathcal{X}$ and given by:

$$U^b_\mathcal{X} = \min\left(U^b \iint_{\mathcal{A}_\mathcal{X}} f(x, y, b)\ \mathrm{d}x\mathrm{d}y, \bar{U}_\mathcal{X}\right), \quad (1)$$

for MBSs and DBSs, i.e., $\mathcal{X} \in \{m_k, (d_l, i)\}$ and,

$$U^b_0 = \min\left(U^b - \sum_{k=1}^{M} \pi^b_{m_k} U^b_{m_k} - \sum_{l=1}^{D}\sum_{i=1}^{Z} \epsilon^b_{d_l}(i) U^b_{d_l,i}, \bar{U}_0\right), \quad (2)$$

for macrocell BS, i.e, $\mathcal{X} = 0$.

where min is the minimum function.

B. Channel Model

In this paper, we distinguish two channel models depending on the nature of the transmitter.

1) Ground-to-Ground Channel Model: The average path loss (PL) between a ground BS $\mathcal{X} \in \{0, m_k\}$ and a ground user is given by the average PL for non-line of sight (NLoS) links and expressed as [11]:

$$PL^{\text{NLoS}}_\mathcal{X}[\text{dB}] = 20 \log_{10}\left(\frac{4\pi\delta_\mathcal{X}}{\lambda_0}\right) + \xi_{\text{NLoS}}, \quad (3)$$

where $\delta_\mathcal{X}$ is the average distance between the ground BS $\mathcal{X}$ and a served user located within its cell, λ_0 is the carrier wavelength, and ξ_{NLoS} is the average additional loss due to the free space propagation loss for NLoS link.

2) Air-to-Ground Channel Model: The PL of air-to-ground link is a weighted combination of two PL links: LoS and NLoS links. This is due to the mobility and ability of drones to serve users from high altitude as compared to ground BSs. In this case, there will be a probability to obtain a LoS link between the DBS and a user [11]. The average PL between the DBS l positioned at a position i and a served user in urban environments for line of sight (LoS) is given as [11]:

$$PL_{d_l,i}^{\text{LoS}}[\text{dB}] = 20\log_{10}\left(\frac{4\pi\delta_{d_l,i}}{\lambda_0}\right) + \xi_{\text{LoS}}, \tag{4}$$

where δ_{d_l} is the average distance between the DBS l and the served user located in its cell and ξ_{LOS} is the average additional loss to the free space propagation loss for LoS link.

The LoS probability is given by [4], [12], [13]:

$$p_{d_l,i}^{\text{LoS}} = \frac{1}{1+\nu_1\exp(-\nu_1[\theta_{d_l,i}-\nu_2])}, \tag{5}$$

where $\theta_{d_l,i}$ is the elevation angle between DBS l positioned at location i and the served user in (degree). ν_1 and ν_2 are constant values that depend on the environment. The NLoS probability is, then, equal to $1-p_{d_l,i}^{\text{LOS}}$. Therefore, the average PL for air-to-ground link is given by:

$$\overline{PL}_{d_l,i} = p_{d_l,i}^{\text{LoS}} PL_{d_l,i}^{\text{LoS}} + (1-p_{d_l,i}^{\text{LoS}}) PL_{d_l,i}^{\text{NLoS}}. \tag{6}$$

C. Base Stations Power Model

In the active state, to serve its connected users during a time block b, the BS $\mathcal{X}$ consumes a power denoted by $P_{\mathcal{X}}^b$, however, in the idle mode, it consumes a constant power equal to $P_{\mathcal{X}}^{\text{idle}} = \gamma_{\mathcal{X}}$. The latter power corresponds to the minimum power required to readily activate BS $\mathcal{X}$. For simplicity, the total power consumption of an active BS $\mathcal{X}$ during a time block b can be approximated by a linear model as follows [14]:

$$P_{\mathcal{X}}^b = \alpha_{\mathcal{X}}\tilde{P}_{\mathcal{X}}^b + \beta_{\mathcal{X}}, \tag{7}$$

where $\alpha_{\mathcal{X}}$ is the scaling parameter and $\beta_{\mathcal{X}}$ models an offset of site power which is consumed independently of the average radiated power of BS which is denoted by $\tilde{P}_{\mathcal{X}}^b$ and expressed as:

$$\tilde{P}_{\mathcal{X}}^b = U_{\mathcal{X}}^b P_{\min}\overline{PL}_{\mathcal{X}}, \tag{8}$$

where $\overline{PL}_{\mathcal{X}}$ is the corresponding average PL of the BS $\mathcal{X}$. Note that $\overline{PL}_{\mathcal{X}} = PL_{\mathcal{X}}^{\text{NLoS}}$ given in (3) in the case of a macrocell BS or MBS and $\overline{PL}_{\mathcal{X}} = \overline{PL}_{d_l,i}$ given in (6) in case of a DBS.

D. Drone Power Model

Besides the power consumed by the BSs carried by the drones (i.e., DBSs), the drone consumes additional hovering and hardware powers. Without loss of generality, we assume that all drones move with a fixed speed denoted by v_d. The hover and hardware drone power levels, denoted by P_{hov} and P_{har}, can be expressed, respectively, as [15]:

$$P_{\text{hov}} = \sqrt{\frac{(m_{\text{tot}}g)^3}{2\pi r_p^2 n_p \rho}}, \text{ and } P_{\text{har}} = \frac{P_{\text{full}}-P_s}{v_{\max}}v_d + P_s, \tag{9}$$

where m_{tot}, g, and ρ are the drone mass in (Kg), earth gravity in (m/s^2), and air density in (Kg/m^3), respectively. r_p and n_p are the radius and the number of the drone's propellers, respectively. $v_{\max}$ is the maximum speed of the drone. P_{full} and P_s are the hardware power levels when the drone is moving at full speed and when the drone is in idle mode, respectively. Note that in (9) we assume that when serving users at a location i, the drone will be in a static position, hence, it consumes only P_s for hardware power. However, when it is flying to a destination (i.e., one of the $Z+1$ locations), it will consume P_{har}. Finally, the flying power of DBS l can be calculated as:

$$P_f = P_{\text{hov}} + P_{\text{har}}. \tag{10}$$

E. Renewable Energy Model

In this paper, we assume that DBS l can harvest from renewable energy (RE) sources selected to be the photovoltaic energy. We model the RE stochastic energy arrival rate as a random variable Φ Watt defined by a pdf $g(\varphi_{d_l}^b)$. An event $\eta\varphi_{d_l}^b$ in a time block b can be interpreted as the average received amount of power with respect to the received luminous intensity in a particular direction per unit solid angle. η denotes the EH efficiency coefficient.

To summarize, we present in Table I the consumed and harvested energies of the drone for all possible scenarios: 1) when the drone is at a location other than location $i \neq 0$ at time block $b-1$, 2) when the drone remains at the same location $i \neq 0$, 3) when the drone decides to go to the charging station (i.e., $i=0$) while it was positioned at location $j \neq 0$ during block $b-1$, and 4) when the drone decides to stay in the charging station $i=0$. In Table I, $T_f(j,i)$ corresponds to the drone trip duration from a location j to a location i while $T_r(j,i) = T_b - T_f(j,i)$ and it corresponds to the time spent by a drone at a location i to serve users (i.e., $i \neq 0$) or charge its battery (i.e., $i=0$) with $T_f(j,i) \ll T_b$. P_{ch} denotes the power per drone of the charging station.

III. Problem Formulation

In this section, we formulate two optimization problems aiming to minimize the network's energy consumption during the B time blocks. Choosing this metric reduces at maximum the use of drones and hence send them only when needed. The first one corresponds to an online scenario where the mobile operator manages its BSs time block by time block due to limited information about the future traffic and RE generation. The second one considers full knowledge of the future statistics and hence, optimizes all the decisions variables simultaneously for the B time blocks.

A. Online Optimization

The total energy consumption of the network during time block b can be expressed as:

$$E_{\text{tot}}^b = E_0^b + E_M^b + E_D^b, \tag{11}$$

where, using (2) and (7), $E_0^b = \left(\alpha_0\tilde{P}_0^b\left(\boldsymbol{\pi}^b, \boldsymbol{\epsilon}^b\right) + \beta_0\right)T_b$ and represents the energy consumption of the macrocell BS during

Table I: Consumed and harvested energies of DBS l during a time block b for all possible cases

Previous location	Current location	Consumed energy	Harvested energy	Charging energy
$\epsilon_{d_l}^{b-1}(j)=1,\, j\neq i$	$\epsilon_{d_l}^{b}(i)=1,\, i\neq 0$	$(P_f+\gamma_d)T_f(j,i)+(P_{d_l,i}^b+P_s)T_r(j,i)$	$\eta\varphi_{d_l}^b(T_f(j,i)+T_r(j,i))$	0
$\epsilon_{d_l}^{b-1}(j)=1,\, j=i$	$\epsilon_{d_l}^{b}(i)=1,\, i\neq 0$	$(P_{d_l,i}^b+P_s)T_b$	$\eta\varphi_{d_l}^b T_b$	0
$\epsilon_{d_l}^{b-1}(j)=1,\, j\neq 0$	$\epsilon_{d_l}^{b}(i)=1,\, i=0$	$(P_f+\gamma_d)T_f(j,i)+\gamma_d T_r(j,i)$	$\eta\varphi_{d_l}^b(T_f(j,i)+T_r(j,i))$	$P_{ch}T_r(j,i)$
$\epsilon_{d_l}^{b-1}(j)=1,\, j=0$	$\epsilon_{d_l}^{b}(i)=1,\, i=0$	$\gamma_d T_b$	$\eta\varphi_{d_l}^b T_b$	$P_{ch}T_b$

time block b. E_M^b is the total energy consumption of M MBSs during time block b which is expressed as:

$$E_M^b=\sum_{k=1}^{M}\left[\pi_{m_k}^b(\alpha_m\tilde{P}_{m_k}^b+\beta_m)+(1-\pi_{m_k}^b)\gamma_m\right]T_b. \quad (12)$$

Finally, $E_D^b=\sum_{l=1}^{D}E_{d_l}^b$ corresponds to the total energy consumption of all drones D during time block b. Using Table I and knowing that $T_f(i,i)=0$, the total energy consumption of a drone d_l during time block b is expressed as follows:

$$E_{d_l}^b=\epsilon_{d_l}^b(0)\sum_{j=0}^{Z}\epsilon_{d_l}^{b-1}(j)\left[(P_f+\gamma_d)T_f(j,0)+\gamma_d T_r(j,0)\right]+\sum_{i=1}^{Z}\sum_{j=0}^{Z}\epsilon_{d_l}^b(i)\epsilon_{d_l}^{b-1}(j)\left[(P_f+\gamma_d)T_f(j,i)+(P_{d_l}+P_s)T_r(j,i)\right]. \quad (13)$$

On the other hand and again using Table I, the total harvest-plus-charging energy of DBS l during time block b due to EH and P_{ch}, denoted by $H_{d_l}^b$, is given as follows:

$$H_{d_l}^b=\epsilon_{d_l}^b(0)\sum_{j=0}^{Z}\epsilon_{d_l}^{b-1}(j)\left[\eta\varphi_{d_l}^b T_f(j,0)+(\eta\varphi_{d_l}^b+P_{ch})T_r(j,0)\right]+\sum_{i=1}^{Z}\sum_{j=0}^{Z}\epsilon_{d_l}^b(i)\epsilon_{d_l}^{b-1}(j)\eta\varphi_{d_l}^b\left[T_b\right]. \quad (14)$$

The stored energy by DBS l at the end of time block b, denoted by $S_{d_l}^b$, is given as by:

$$S_{d_l}^b=S_{d_l}^{b-1}+H_{d_l}^b-E_{d_l}^b. \quad (15)$$

We assume that initially each battery is charged by an amount of energy denoted by $S_{d_l}^0$. Hence, the optimization problem minimizing the total energy consumption at each time block b with EH drones is given as:

$$\underset{\boldsymbol{\epsilon}^b\in\{0,1\},\boldsymbol{\pi}^b\in\{0,1\}}{\text{minimize}} \quad E_{\text{tot}}^b=E_0^b+E_M^b+E_D^b \quad (16)$$

subject to:

$$E_{d_l}^b\leq S_{d_l}^{b-1},\quad \forall l, \quad (17)$$

$$S_{d_l}^{b-1}+H_{d_l}^b\leq\bar{S},\quad \forall l, \quad (18)$$

$$\sum_{i=0}^{Z}\epsilon_{d_l}^b(i)=1,\quad \forall l, \quad (19)$$

$$\sum_{l=1}^{D}\epsilon_{d_l}^b(i)\leq 1,\quad \forall i=1,\cdots,Z, \quad (20)$$

$$U^b-\sum_{k=1}^{M}\pi_{m_k}^b U_{m_k}^b-\sum_{l=1}^{D}\sum_{i=1}^{Z}\epsilon_{d_l}^b(i)U_{d_l,i}^b\leq\bar{U}_0, \quad (21)$$

Constraint (17) indicates that the total energy consumed by a drone d_l during the time block b has to be less than the energy stored at the beginning of this time block. Constraint (18) forces the total energy stored in the battery of a drone d_l during the time block b to be less than the battery capacity denoted by $\bar{S}$. Note that $\bar{S}$ is chosen such that the required energy to return a drone to the charging station ($i=0$) is guaranteed. This energy is simply equal to $P_f T_f(i_{\max},0)$ where $i_{\max}$ the farthest location from $i=0$. Constraints (19) and (20) prevent the optimization problem from positioning a drone in two or more different locations during the same time block and positioning at maximum one drone in the locations $i=1,\cdots,Z$, respectively. Multiple drones can be located simultaneously at the charging station $i=0$. Finally, constraint (21) ensures that the macrocell BS's capacity is not violated. This constraint encourages the activation of MBSs and the deployment of DBSs during high traffic time blocks.

Notice that this optimization problem will be solved at the beginning of each time block which is possible due to the knowledge of the status of the network during the previous time block $\boldsymbol{\epsilon_{b-1}}$. Hence, the problem can be converted to the standard form of a binary linear programming optimization problem and the decision variables can be re-written in a single vector $\boldsymbol{W}=\left[\epsilon_1^b(0),\cdots,\epsilon_1^b(Z)\epsilon_2^b(0),\cdots\cdots,\epsilon_D^b(Z),\pi_1^b,\cdots,\pi_M^b\right]$. Optimal solutions for such a problem can be determined using Cplex [16].

B. Offline Optimization

In this case, the objective function becomes the minimization of the total energy consumption of the network during all B time blocks. The decision variables are identified as $\boldsymbol{\epsilon}$ and $\boldsymbol{\pi}$ that correspond to the vertical concatenation of the matrices $\boldsymbol{\epsilon}^b$ and $\boldsymbol{\pi}^b,\forall b=1,\cdots,B$, respectively. Hence, the problem becomes a binary non-linear programming problem due to the existence of the binary products $\epsilon_{d_l}^{b-1}(j)\epsilon_{d_l}^b(i)$ in the energy expressions given in (13) and (14). To linearize the problem, we introduce for each link the parameter $\zeta_{d_l}^b(j,i)$ such that $\zeta_{d_l}^b(j,i)=\epsilon_{d_l}^{b-1}(j)\epsilon_{d_l}^b(i)$ where the following inequalities have to be respected:

$$\zeta_{d_l}^b(j,i)\leq\epsilon_{d_l}^{b-1}(j),\quad \zeta_{d_l}^b(j,i)\leq\epsilon_{d_l}^b(i),\quad \text{and } \zeta_{d_l}^b(j,i)\leq\epsilon_{d_l}^{b-1}(j)+\epsilon_{d_l}^b(i)-1. \quad (22)$$

The first two inequalities ensure that $\zeta_{d_l}^b(j,i)=0$ if $\epsilon_{d_l}^{b-1}(j)$ or $\epsilon_{d_l}^b(i)$ is zero. The third inequality guarantees that $\zeta_{d_l}^b(j,i)=1$ if $\epsilon_{d_l}^{b-1}(j)=\epsilon_{d_l}^b(i)=1$. Hence, the expressions (13) and (14) become depending on $\zeta_b(d_l,n)$ and the decision variables turn into $\boldsymbol{\zeta}$, $\boldsymbol{\epsilon}$, and $\boldsymbol{\pi}$ that have the following number of elements: $BD(Z+1)^2$, $BD(Z+1)$, and BM, respectively. Accordingly, the optimization problem that minimizes the network energy consumption during all B time blocks is given by:

$$\underset{\substack{\boldsymbol{\epsilon}\in\{0,1\},\boldsymbol{\pi}\in\{0,1\},\\ \boldsymbol{\zeta}\in\{0,1\}}}{\text{minimize}} \quad E_{\text{tot}} = \sum_{b=1}^{B} E_0^b + E_M^b + E_D^b \tag{23}$$

subject to:

$$\sum_{t=1}^{b} E_{d_l}^t - \sum_{t=1}^{b-1} H_{d_l}^t \leq S_{d_l}^0, \quad \forall l, \forall b, \tag{24}$$

$$S_{d_l}^0 + \sum_{t=1}^{b} H_{d_l}^t - \sum_{t=1}^{b-1} E_{d_l}^t \leq \bar{S}, \forall l, \forall b, \tag{25}$$

$$\sum_{i=0}^{Z} \epsilon_{d_l}^b(i) = 1, \quad \forall l, \forall b, \tag{26}$$

$$\sum_{l=1}^{D} \epsilon_{d_l}^b(i) \leq 1, \quad \forall i = 1, \cdots, Z, \forall b, \tag{27}$$

$$U^b - \sum_{k=1}^{M} \pi_{m_k}^b U_{m_k}^b - \sum_{l=1}^{D}\sum_{i=1}^{Z} \epsilon_{d_l}^b(i) U_{d_l,i}^b \leq \bar{U}_0, \quad \forall b, \tag{28}$$

$$\zeta_{d_l}^b(j,i) \leq \epsilon_{d_l}^b(i), \quad \forall l, \forall i, \forall j, \forall b, \tag{29}$$

$$\zeta_{d_l}^b(j,i) \leq \epsilon_{d_l}^{b-1}(j), \quad \forall l, \forall i, \forall j, \forall b, \tag{30}$$

$$\zeta_{d_l}^b(j,i) \geq \epsilon_{d_l}^{b-1}(j) + \epsilon_{d_l}^b(i) - 1, \quad \forall l, \forall i, \forall j, \forall b, \tag{31}$$

Notice that the constraints (24)-(28) are similar to the constraints (17)-(21) except that they have to be satisfied for all time blocks $b = 1, \cdots, B$. The constraints (24)-(25) are obtained by replacing $S_{d_l}^b$ by its expression given in (15). The constraints (29)-(31) correspond to the linearization process as indicated in (22). In terms of complexity, the linearized offline optimization problem is largely more complex than the online one due to the higher number of binary decision variables and constraints. The linearized offline problem can be also solved using Cplex.

IV. Selected Numerical Results

In this section, selected numerical results are provided to investigate the benefits of utilizing dynamic DBSs in HetNets. We assume a HetNet consisting of one macrocell BS with radius of one km, four MBSs ($M = 4$) with a coverage of 250 meters, and six identical drones ($D = 6$), unless otherwise stated, that can potentially placed in sixteen different locations ($Z = 16$) with same altitude $h_i = 60$, meters, $\forall i = 1, \ldots, 16$ and a coverage of 150 meters. The Z pre-planned locations are indicated as depicted in Fig 2. We assume that the drones are initially charged with $S_{d_l}^0 = 6$ kJ of energy and placed at the charging station. The average received amount of photovoltaic power $\phi_{d_l}^b$ is assumed to be generated following a Gamma distribution with shape and scale parameters equal to 1 and 2, respectively. We assume that $U^b = 140, \forall b = 1, \cdots, B$ users exist within the macrocell. In case of overlap between the micro cell and an active DBS, we assume that the drone has the priority in serving the users in the intersection region once deployed. In Table II, we present the values of the remaining parameters used in the simulations [14], [15].

In Fig. 2, we start by investigating the behavior of two selected drones, namely drone d_1 and drone d_3 respectively, for two different user distribution but same number of users and RE generation per drone and time block. In Fig. 2(a,c), we consider a uniform user distribution and hence, if a drone is placed in a location $i \neq 0$, it will serve exactly the same number of users as another drone placed in another location $j \neq i$. In Fig. 2(b,d), another non-uniform distribution is considered where the number of users to be served differs from a location to another. It is shown that with uniform distribution, once the drone is sent to a location i then it has two possibilities for the next block, either to stay at the same location (e.g., d_1 during $b = 3, 4$) if it has enough energy or return back to the charge station (e.g., d_1 during $b = 2$). On the other hand, with the random distribution, the drone can go from one location to another to serve the users without passing by the charging station. For instance, d_1 goes to $i = 5$ in $b = 3$, then moves to $i = 2$. It is also worth to note that the drones avoid long distance trip when selecting the locations unless they are forced to do due to high user density in these locations (e.g., d_3 with random distribution moves to $i = 2, 15$ during $b = 3, 1$ and 5).

Table II: System parameters

Parameter	Value	Parameter	Value	Parameter	Value
λ (m)	0.125	$P_{\min}(dBm)$	-70	T_b	10
ν_1	9.6	ν_2	0.29	ξ_{LoS} (dB)	1
ξ_{NLoS} (dB)	12	α_0	4.7	β_0 (W)	130
α_m	2.6	β_m (W)	56	γ_m (W)	39
α_d	4	β_d (W)	6.8	γ_d (W)	2.9
S (kJ)	10	$v_d = v_{\max}$ (m/s)	15	m_{tot} (g)	750
r_p (cm)	20	n_p	4	P_s (W)	0.5
P_{ch} (W)	10	η	0.9	U_0	130

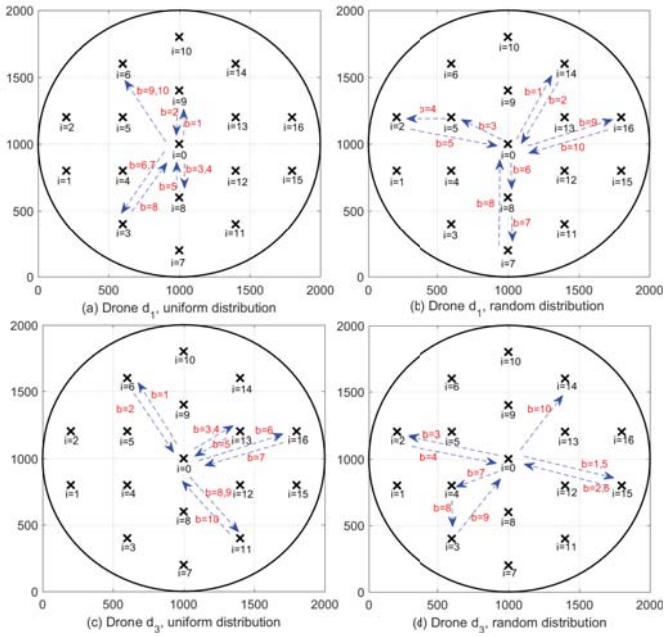

Fig. 2: The behavior of two drones, drone d_1 (a,b), drone d_3 (c,d) for different user distributions with $D = 6$.

In Fig. 3, we plot the energy consumption and number of active drones for $B = 20$ time blocks and different number of users uniformly distributed (i.e., $U^b = 140$ and $U^b = 160, \forall b$). This figure investigates the impact of RE for two cases: 1) when the drones are supported by solar panel (blue lines) and 2) when the drones are charged by the central station only (red line). It is shown that EH don't only reduce the

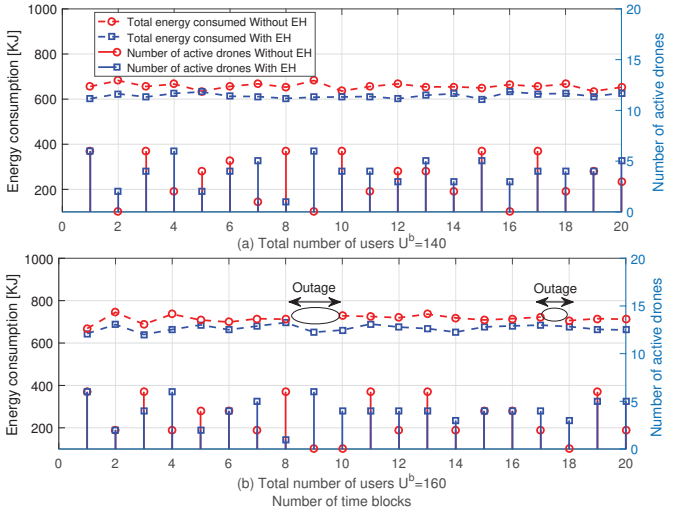

Fig. 3: Total energy consumption and number of active drones during the trial period.

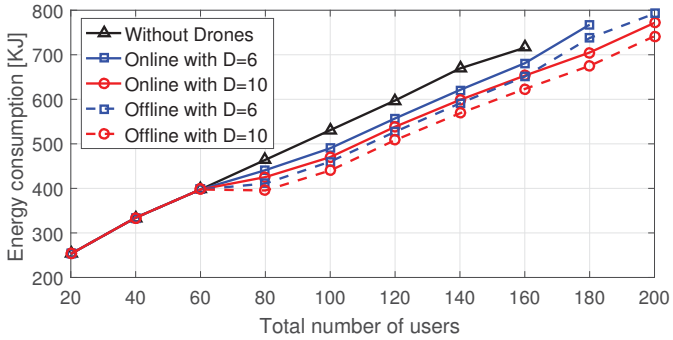

Fig. 4: A comparison between the online and offline methods for different values of D .

total energy consumption of the network but also, help in avoiding (or decreasing) the outage risk (i.e., where not all users can be simultaneously served). Indeed, when the number of users in the network is relatively large (e.g., U^b=160), two outage periods are detected $b = \{9, 10\}$ and $b = 18$. This outage is due to two reasons. Firstly, the non-EH drones need to go more frequently to the central station than the drones supported by EH to charge their batteries. Secondly, the EH drones can harvest energy when flying and serving users which contributes to increase the battery level and hence, get more flexibility to move to other locations without passing by the charging station. This is deduced from the number of active drones of each case.

Finally, Fig. 4 compares between the online and offline methods presented in Section. III for different number of drones while increasing the total number of users per time block. It is noticed that increasing the number of drones help in avoiding network outage and reducing the total energy consumption specially when the network becomes more and more congested. Furthermore, the offline method achieves a more important energy saving due to its efficient management of the harvested energy compared to the online method. Nevertheless, the achieved performance of the online method follows the same trend of the perfect knowledge method with a minor gap.

V. Conclusions

In this paper, we proposed an energy management framework for cellular heterogeneous networks assisted by solar-powered drone small cells. The objective is to minimize the total energy consumption of the networks while maintaining the network coverage and connectivity during low and high traffic periods. Drone base stations are optimally managed in order to support the overloaded cells while considering their photovoltaic energy generation and battery capacity. Results show the behavior of dynamic drones in a time-blocked system and their significant impacts on ensuring connectivity with minimum energy consumption.

References

[1] I. Bucaille et al., "Rapidly deployable network for tactical applications: Aerial base station with opportunistic links for unattended and temporary events absolute example," in *IEEE Military Communications Conference (MILCOM)*, Nov. 2013, pp. 1116–1120.

[2] S. Rohde and C. Wietfeld, "Interference aware positioning of aerial relays for cell overload and outage compensation," in *IEEE Vehicular Technology Conference (VTC Fall), Quebec, QC, Canada*, Sept. 2012, pp. 1–5.

[3] P. Zhan, K. Yu, and A. L. Swindlehurst, "Wireless relay communications using ann unmanned aerial vehicle," in *IEEE Workshop on Signal Processing Advances in Wireless Communications, Cannes, France*, July 2006, pp. 1–5.

[4] M. Mozaffari, W. Saad, M. Bennis, and M. Debbah, "Drone small cells in the clouds: Design, deployment and performance analysis," in *IEEE Global Communications Conference (GLOBECOM), San diego, CA, USA*, Dec. 2015, pp. 1–6.

[5] J. Xu and R. Zhang, "Throughput optimal policies for energy harvesting wireless transmitters with non-ideal circuit power," *IEEE Journal on Slected Areas in Communications*, vol. 32, no. 2, pp. 322–332, Feb. 2014.

[6] H. Tabassum, E. Hossain, A. Ogundipe, and D. I. Kim, "Wireless-powered cellular networks: Key challenges and solution techniques," *IEEE Communications Magazine*, vol. 53, no. 6, pp. 63–71, June 2015.

[7] S. Ulukus, A. Yener, E. Erkip, O. Simeone, M. Zorzi, P. Grover, and K. Huang, "Energy harvesting wireless communications: A review of recent advances," *IEEE Journal on Selected Areas in Communications*, vol. 33, no. 3, pp. 360–381, Mar. 2015.

[8] Z. Hasan, H. Boostanimehr, and V. Bhargava, "Green cellular networks: A survey, some research issues and challenges," *IEEE Communications Surveys & Tutorials*, vol. 13, no. 4, pp. 524–540, Fourth 2011.

[9] V. Raghunathan, S. Ganeriwal, and M. Srivastava, "Emerging techniques for long lived wireless sensor networks," *IEEE Communications Magazine*, vol. 44, no. 4, pp. 108–114, Apr. 2006.

[10] C. Liu, B. Natarajan, and H. Xia, "Small cell base station sleep strategies for energy efficiency," *IEEE Transactions on Vehicular Technology*, vol. 65, no. 3, pp. 1652–1661, Mar. 2016.

[11] A. Al-Hourani, S. Kandeepan, and A. Jamalipour, "Modeling air-to-ground path loss for low altitude platforms in urban environments," in *IEEE Global Communications Conference (GLOBECOM), Austin, TX, USA*, Dec. 2014, pp. 2898–2904.

[12] Y. W. Y. Zheng and F. Meng, "Modeling and simulation of pathloss and fading for air-ground link of haps within a network simulator," in *IEEE International Conference on Cyber-Enabled Distributed Computing and Knowledge Discovery (CyberC), Beijing, China*, Oct. 2013.

[13] A. Al-Hourani, S. Kandeepan, and S. Lardner, "Optimal LAP altitude for maximum coverage," *IEEE Wireless Communications Letters*, vol. 3, no. 6, pp. 569–572, Dec. 2014.

[14] "Energy efficiency analysis of the reference systems, areas of improvements and target breakdown," *Energy Aware Radio and neTwork tecHnologies*, Dec. 2010.

[15] J. V. Dries Hulens1 and T. Goedeme, "How to choose the best embedded processing platform for onboard UAV image processing," in *Proc. of the International Joint Conference Computer Vision, Imaging and Computer Graphics Theory and Applications (VISIGRAPP), Berlin, Germany*, Mar. 2015.

[16] R. Zakaria, M. Dib, L. Moalic, and A. Caminada, "Car relocation for carsharing service: Comparison of CPLEX and greedy search," in *Proc. of the IEEE Symposium on Computational Intelligence in Vehicles and Transportation Systems, Orlando, Florida, USA*, Dec. 2014, pp. 51–58.